Environmental and Climate Technologies
2025, vol. 29, no. 1, pp. 259–271
https://doi.org/10.2478/rtuect-2025-0018
https://content.sciendo.com

5th Generation District Heating and Cooling (5GDHC) Systems: Improving the Efficiency of a Booster Heat Pump

Stanislav CHICHERIN[1*], Jonathan HACHEZ[2], Afraz Mehmood CHAUDHRY[3], Svend BRAM[4]

[1,2,4]*Thermo and Fluid Dynamics (FLOW), Faculty of Engineering, Vrije Universiteit Brussel (VUB), Pleinlaan 2, 1050 Brussels, Belgium*

[1,2,4]*Brussels Institute for Thermal-Fluid Systems and Clean Energy (BRITE), Vrije Universiteit Brussel (VUB) and Université Libre de Bruxelles (ULB), 1050 Brussels, Belgium.*

[3]*Energy Efficient & Resilient Built Environment, CENAERO, Bâtiment Eole, Rue des Frères Wright, 29, 6041 Gosselies, Belgium*

Received 10.03.2025; accepted 04.05.2025

***Abstract* – This study addresses the limitations of booster heat pumps in achieving high secondary supply temperatures, which are constrained by declining Carnot efficiency. The research investigates the performance and economic feasibility of integrating booster water-to-water heat pumps into a 5th generation district heating and cooling (5GDHC) system, particularly for a newly built office building in a moderate climate zone with an average winter supply temperature of 50 °C. The methodological framework assumes idealized system behavior without part-load penalties, and models heat pump performance based on Carnot cycle efficiency corrected by a typical Carnot scaling factor ($\eta = 0.6$). Key assumptions include fixed building envelope characteristics, specific energy consumption based on energy performance certificates, and cost parameters for standard and advanced heat pumps (1.5× and 5× higher variable and fixed costs, respectively). The model incorporates pinch temperatures to reflect practical heat exchange limitations and applies a simultaneity factor for accurate heat pump sizing across multiple buildings. Results show that despite a 50 % increase in capital expenditures (CapEx), operational expenditures (OpEx) decrease significantly, resulting in an overall cost reduction of 11 %. Advanced heat pumps with 22 % higher efficiency compared to mass-market units demonstrate notable improvements in seasonal COP (SCOP) by 22 % and electricity consumption by 18 %. Maximum COPs of 6.0 in winter and 12.0 in transitional periods are observed. A peak heat demand of 12 MW is covered by 25 booster units averaging 478 kW each, activated when secondary supply temperatures exceed the network temperature. The findings support the strategic deployment of efficient, electricity-driven booster heat pumps in 5GDHC systems. Improved thermal integration and the use of renewable energy sources further reduce energy costs and carbon emissions, enhancing both the energetic and economic performance of the system.**

***Keywords* – Carnot; COP (coefficient of performance); costs; investments; substation.**

* Corresponding author.
E-mail address: stanislav.chicherin@vub.be

1. Introduction

A booster heat pump can improve the system's heating performance by 50 % compared to a traditional individual heat pump heating system [1]. Their efficiency is much higher than that of ground-source heat pumps. They have a high geo-exchange potential ensured by conduction and convection, but use water in the boreholes with temperatures ranging between 5–15 °C only. Placing boreholes is well-covered by existing research. For instance, in [2], ranges of 0–150 m and 0–200 m are considered, and when compared, the 0–200 m is better in conductive, convective, and temperature terms. Both the booster and ground-source heat pumps are typical and equal components of a multi-energy system, although the former is studied much less. Another example of a multi-energy system, including heat pumps, is presented in [3]. Their case study is Helsinki City (Finland), where four main districts are considered: Helsinki 1, Helsinki 2, Espoo, and Vantaa. COP for one heat pump achieves 5.2, although for some heat pumps, it is 3.0 only.

Calise *et al.* [4] present a multi-energy system comprising heat and electricity subsystems. There are at least seven separate conduits, all ensuring heat flow but with different energy potentials, including open-loop sea water, closed-loop water, domestic hot water, district cooling, district heating, etc. Key components are pipes, heat exchangers, and heat pumps. To run such a system, working on both direct and alternating current due to the public grid, photovoltaic field, and wind turbines involved, diverters, inverters, and regulators are necessary.

Sorknaes *et al.* [5] present an even more complex multi-energy system with two types of heat pumps included: electricity-driven and absorption ones, see Fig. 1.

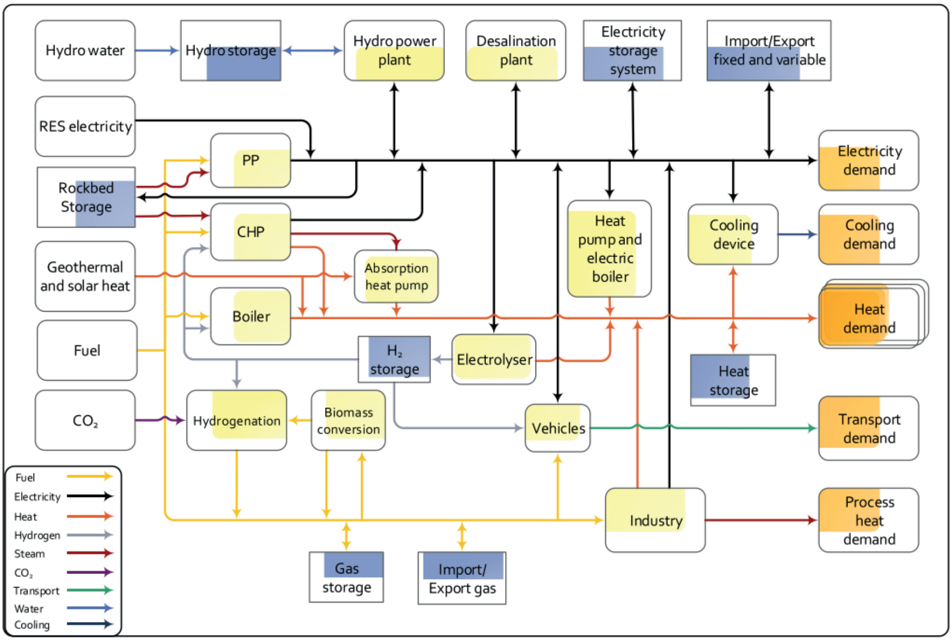

Fig. 1. An example of a multi-energy system considered in [5]. Adopted from [5].

Fig. 1 illustrates a complex, integrated energy system. While it does not explicitly show a booster heat pump, it highlights such a device's role within a broader energy system. For instance, this research directly addresses how to meet "Heat demand" (orange box) efficiently, particularly for space heating in an office building requiring a high secondary supply temperature (50 °C). "Heat pump and electric boiler" (another yellow box) are the competing technologies to meet this heating demand. This research highlights the substantial benefits of using more advanced, higher-efficiency heat pump technologies, although they can be costly.

"Heat storage" (blue) may affect the operational strategy of a booster heat pump. For instance, heat can be stored during periods of lower demand or higher efficiency and then used to supplement the booster pumps during peak times. The same goes for the primary energy side, which is marked as unfilled boxes. Integrating "Geothermal and solar heat" with more efficient heat pumps may significantly impact the overall efficiency and the response to the system demand. In turn, that may veer future research from storage and networks that are typically the most cost-intensive investments. If the network is powered by renewable electricity, see "Hydro power plant" (yellow box) or "RES electricity" (grey box), the environmental benefits of a more efficient heat pump system are amplified.

There are two more examples of such linked connections: "CHP" (yellow box) & "Boiler" (yellow box) using "Fuel" (grey box): if the 5th generation district heating and cooling (5GDHC) network relies on fossil fuels as auxiliary source, the efficiency gains from heat pumps become even more critical for reducing emissions and operational costs; "Industry" (yellow box) & "Process heat demand" (orange box): less waste heat recovery from industrial processes is necessary as a low-temperature source for more-efficient booster heat pumps.

Cozzini *et al.* [6] present the COP for different modes of heat pump operation. As a benchmark, they use Aermec WRL 081 heat pump model, and by obtaining a similar COP of 4–5 for the same condenser and evaporator temperature, they corroborate the findings presented in this paper for the business-as-usual scenario.

To utilize solar energy, Brunt *et al.* [7] install a collector and a heat pump at the decentralized level. Two more heat pumps are installed at the central plant. To cover the gap between heat demand and energy production, they install two hot water tanks; when they are not enough, an auxiliary boiler is in operation.

Al-Sayyab *et al.* [8] suggest a novel solar-driven ejector-compression system. Its key component is an ejector, which ensures flow mixing and water circulation in a space heating system without a pump, provided the mixed flows have been pressurized before. Dino *et al.* [9] present the substation configuration for a prosumer in a 5GDHC system. It includes 3 heat exchangers and some valves separating the system into 4 independent hydraulic circuits. Their research emphasized not improving the 5GDHC system by increasing Carnot efficiency but suggesting a new configuration of the substation, including a booster heat pump, as an unchanged unit.

To compare, Capone *et al.* [10] study one DH system only, and based on the indicators of the annual operation, they indicate the best position for a heat pump. In their case, the effect of installing the heat pump in its optimal position is much less than those presented here: energy costs decrease from 115 to 111 EUR/MWh only. Apparently, an improvement is not due to the thermal cycle of the heat pump itself but its positioning in the distant network.

In [11], the COP varies according to the system load, reaching 100 % at full load. According to Pasqui *et al.* [11], the maximum possible COP is actually 133 %, which can be achieved at 0.50–0.55 of the full load. To compare, Maccarini *et al.* [12] also present the configuration of the 5GDHC system. It includes a separate heat pump for space heating, a heat pump for domestic hot water, and a heat exchanger for direct cooling. Residential buildings do not have heat exchangers because no cooling is considered. It operates with a lower network supply temperature of 15 °C, limiting the COP for a booster heat pump. Again, no in-depth study of heat pumps is given.

Martinazzoli *et al*. [13] present a configuration distinguishing operation in the heating and cooling modes. The difference is the decentralized pumping system. The heat pump also indicates the refrigerant conditions at the evaporator and condenser inlets and outlets, which is a bit too much into a thermodynamic cycle itself. Gong *et al*. [1] comprehensively review the latest technologies available for 5GDHC. Among them, there are more efficient heat pumps. Despite that, even a traditional booster heat pump system may save up to 725 MWh of electrical energy per year just because it uses a warm pipe of the network rather than outdoor air as a source of low potential energy. Gong *et al*. [1] and Quirosa *et al*. [14] papers contain the ideas directly used for the following study. Therefore, they are discussed in detail in the Results section. In [15], a gradual conversion of the remaining individual heat demand to electrical heat pumps is investigated.

Frik *et al*. [16] addresses the operational optimization of heat pumps within air handling units, seeking to maximize their performance through precise control of thermodynamic processes. This focus on internal efficiency is complemented by Ołtarzewska & Krawczyk [17] who broadens the scope to examine how external climatic factors influence overall heat pump effectiveness across diverse geographical contexts. Finally, Kirs *et al*. [18] offer a system-level perspective, exploring the integration of heat pumps within district energy networks to recover waste heat and improve energy utilization on a city-wide scale. Together, these studies contribute to a more complete understanding of how to improve heat pump technology.

Compared to the present paper and the abovementioned references, Arabkoohsar *et al*. [19] focus mostly on the DHW consumption of the total profile of each neighborhood at any instant, setting its temperature to the constant value of 50 °C. A similar feature is inputting the temperature of return water from each neighborhood of a large district heating system, as implemented in the previous author's paper [20]. Unlike us, Serrat *et al*. [21] consider temperatures applicable for energy storage rather than energy supply. In [21], even in the heating mode, the water comes from the soil at 15 °C and leaves the heat pump at 10 °C. In the cooling mode, the temperatures are closer to those presented in this paper: the water comes from the ground at 25 °C and exits the heat pump at 30 °C. In [22], at any time step, the heat pump simply increases the water temperature from the evaporator to the condenser at the same temperature levels by using electrical power without respect to external or internal factors such as secondary supply temperature or working fluid. The difference with [23] is working with performance maps obtained after characterizing the heat pump performance at several stationary operation points with varying source and supply temperatures.

To the best of the authors' knowledge, even though these technologies exist, inputting Carnot efficiency higher than 0.6 for 5DGHC is not well justified. Higher Carnot efficiency is beneficial and results in higher COP and less power consumption, especially when the heat source temperatures (the outdoor air temperature for air source heat pumps and the brine temperature for ground source heat pumps) and network supply temperatures are fixed. The key difference is that these values vary in most of the papers mentioned above. The contribution to the pool of knowledge is supporting COP higher by 20–25 % based on the reference value reported in the heat pumps, seasonal COP of 5–6, and a negligible rate of thermodynamic losses. The novelty addresses the issues of integrating heat pumps into a low-temperature network, for which high secondary supply temperatures are limited due to a considerable drop in the Carnot efficiency. The aim is to cover the effect of operating conditions on the heat pump efficiency due to the changes in the thermodynamic cycle.

2. Materials and Methods

This study employs a scenario-based analytical approach to evaluate booster heat pumps' technical and economic performance integrated into a 5GDHC system. The primary objective is to assess the trade-offs between capital and operational costs under different heat pump configurations, particularly comparing mass-market and advanced units with improved efficiency. Simplified thermodynamic calculations based on modified Carnot cycle models are used to estimate seasonal performance, supported by empirical relationships for sizing and cost estimations from the literature.

The core performance metric, the COP, is modeled using an ideal Carnot cycle as a reference:

$$\mathrm{COP}_{\mathrm{Carnot}} = \frac{T_{\mathrm{cond}}}{T_{\mathrm{cond}} - T_{\mathrm{evap}}}, \tag{1}$$

where

T_{cond} the condensing (supply) temperature, K;
T_{evap} the evaporating (source) temperature, K.

To account for practical inefficiencies, the real heat pump COP is derived by scaling the Carnot COP with an empirical Carnot efficiency factor:

$$\mathrm{COP}_{\mathrm{HP}} = \eta_{\mathrm{HP}} \cdot \mathrm{COP}_{\mathrm{Carnot}}, \tag{2}$$

where $\eta_{\mathrm{HP}} = 0.6$ for mass-market heat pumps (based on typical performance).

A 22 % higher efficiency is assumed for advanced heat pumps.

A pinch temperature difference is introduced to reflect realistic thermal gradients between the heat pump components and the source/sink, reducing the ideal temperatures used in the calculations.

The building heating demand is calculated using a simplified model that accounts for envelope performance and indoor-outdoor temperature differentials:

$$T_{\mathrm{emit}} = T_{\mathrm{in}} + S \cdot \left(T_{\mathrm{in}} - T_{\mathrm{out}}\right), \tag{3}$$

where

T_{emit} the required secondary supply temperature, K;
T_{in}, T_{out} are indoor and outdoor temperatures, K;
S dimensionless factor reflecting building envelope characteristics.

Heat pump sizing is based on an empirical rule of thumb:

$$P_i = f \cdot A \cdot SFSH_i, \tag{4}$$

where

P_i the peak power at building i, kW;
F the dimensioning factor, W/m²;
A the heated floor area, m²;
$SFSH_i$ the simultaneity factor for space heating.

The simultaneity factor is assessed according to the regression presented in Jebamalai *et al.* [24] and affects the sizing of heat pumps. The simultaneity factor represents the ratio of the maximum coincident demand of a group of consumers to the sum of their individual maximum demands. In essence, it acknowledges that not all consumers will require their peak energy simultaneously. This factor is crucial for accurately sizing energy generation and distribution infrastructure in systems serving multiple users, such as district heating or cooling networks. By accounting for the fact that diverse consumption patterns will likely lead to a lower overall peak demand than the simple sum of individual peaks, the simultaneity factor prevents overestimating necessary capacities. This benefit translates to more cost-effective system design, reduced operational costs, and a more realistic assessment of the actual energy load profiles, ultimately leading to improved efficiency and sustainability of the energy system under study.

Operational expenditures (OpEx) are calculated as:

$$\text{OpEx} = \left(\frac{A \cdot \ \text{EPC}}{\text{SCOP}} \right) \cdot \ e \ , \tag{5}$$

where

EPC specific annual energy use for heating, kWh $\text{yr}^{-1}\ \text{m}^{-2}$;
SCOP the seasonal COP (modeled based on average operating conditions);
e the electricity price, EUR/kWh.

Capital expenditures (CapEx) are estimated using cost regressions detailed in the case study, assuming 20-year equipment lifespans. Total system costs are the sum of annual OpEx and amortized CapEx. Costs, energy use, and performance indicators are compared across multiple configurations (e.g., standard vs. advanced heat pumps, with and without booster units).

Input parameters – including EPC values, electricity prices, equipment costs, and typical COP ranges – are derived from existing literature, manufacturer data, and regulatory standards referenced in the introduction. Building and climate parameters are representative of a newly built office building in a temperate climate zone, with average winter secondary supply temperatures of 50 °C.

3. Case Study

As a case study, a promising site for hosting a 5GDHC system ('AlphaCloud' location in Mechelen, Flanders, Belgium) is considered. The average EPC of the buildings there is 300 kWh/m^{2}y, and the electricity is available at 0.33 EUR/kWh. The s-factor is set to 1.5. The pinch temperature of 5 °C is set according to the average conditions in which a heat pump operates. According to [25], the dimensioning factor f is set to 100 W/m^2 for a well-insulated building, and to 150 W/m^2 for others.

Fig. 2 shows the trend lines for CapEx component as a function of the thermal power of a heat pump.

Scenario#1 implies installing booster heat pumps utilizing the refrigerant R-410A as a working fluid. Current heat pump models are selected as market-average models with a rated efficiency of COP (EN 14511) of 4.18 assessed for the heat pump in the ground-source connection and peak consumption of 18.3 kW. Investment costs for this heat pump are described as per the fixed part (5051 EUR per installation) and the variable component of 103 EUR/kW. This configuration is assumed to have the Carnot efficiency of 0.6.

The new configuration (Scenario #2) is assumed to be 1.5 times more expensive in the variable component (153 EUR/kW) and 5 times more expensive in the fixed one (~25 kEUR per installation) due to potential problems associated with developing technologically new units (new design, procuring and manufacturing new elements, tests, and developing documents for certification, etc.). Filling the heat pump with 50 % propylene/50 % butane or 50 % R1234yf/50 % R1233zd(E) refrigerant is assumed to increase its Carnot efficiency by 22 %, which means 0.732. For this particular case study, the heat demand profiles remain the same.

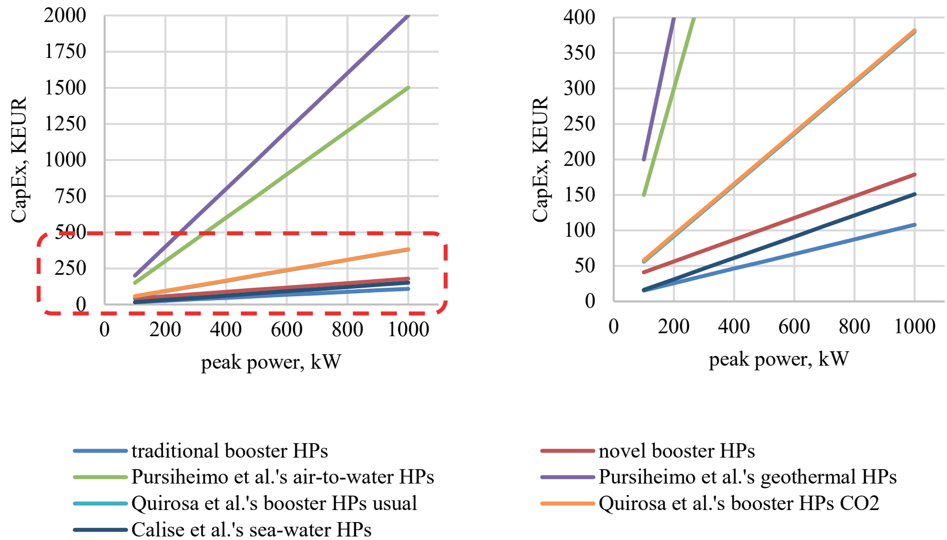

a) b)

Fig. 2. CapEx regression for traditional and novel booster heat pumps (Scenarios #1 and #2, respectively) compared to those given in the literature: a) full range, b) the zone outlined in red, zoomed in.

Regression equations for all the listed curves are presented in Table 1.

TABLE 1. COST COMPONENT COMPARISON (KEUR/KW)

Configuration	**Reference**	**Variable part**	**Fixed part**
Scenario #1 (traditional booster HPs)	n/a	0.103	5051
Scenario #2 (novel booster HPs)	n/a	0.153	25 768
Pursiheimo *et al*. air-to-water HPs	[3]	1.5	n/a
Pursiheimo *et al*. geothermal HPs	[3]	2	n/a
Quirosa *et al*. booster HPs usual	[14]	0.36	20
Quirosa *et al*. booster HPs CO2	[14]	0.36	22
Calise *et al*. sea-water HPs	[4]	0.1497	1.4

4. Results

According to Eq. 3, the secondary supply temperature linearly correlates with the outdoor temperature as seen in Fig. 3.

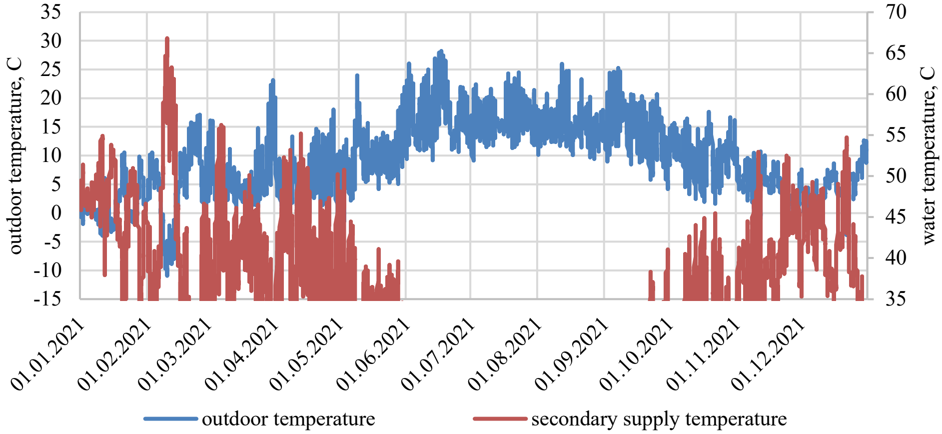

Fig. 3. Secondary supply temperature varies according to the outdoor temperature, reaching a max of 67 °C with an average winter range of 45–55 °C.

According to [1], 50 % propylene/50 % butane or 50 % R1234yf/50% R1233zd(E) refrigerant mixes may considerably enhance the thermodynamic performance of the heat pump unit. These blends are also economically competitive regarding filling and maintenance costs compared to single work gases, and the only problem is their technological implementation. The significant energetic and economic effect of a decoupled strategy for heating and cooling production is also possible with CO_2 booster heat pumps for the 5GDHC system (Fig. 4) [14].

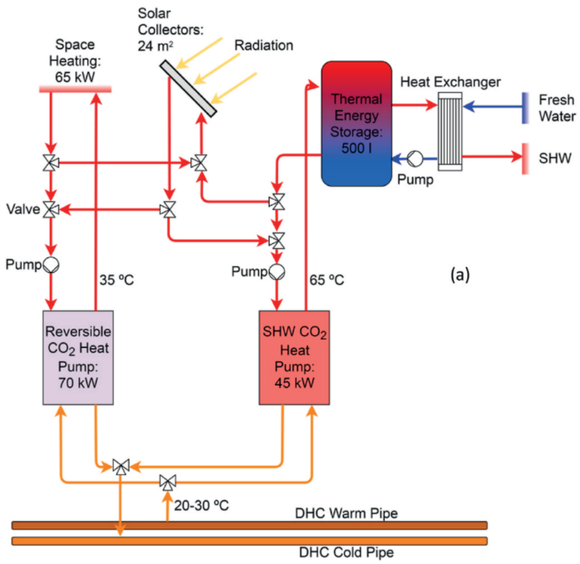

Fig. 4. Solar-driven configuration of a 5GDHC substation. Adopted from [14].

When using the blended masses in both central and booster heat pump units and applied to a 5GDHC system, the range for improvement is between 13 and 22% [1].

By applying these improvements to the 5GDHC system illustrated in the Case study section, two configurations are possible to compare: the first with a mass market water-to-water heat pump and its Carnot efficiency set to 0.6, and the advanced working fluid resulting in 22 % – higher Carnot efficiency (Fig. 5 and Table 2).

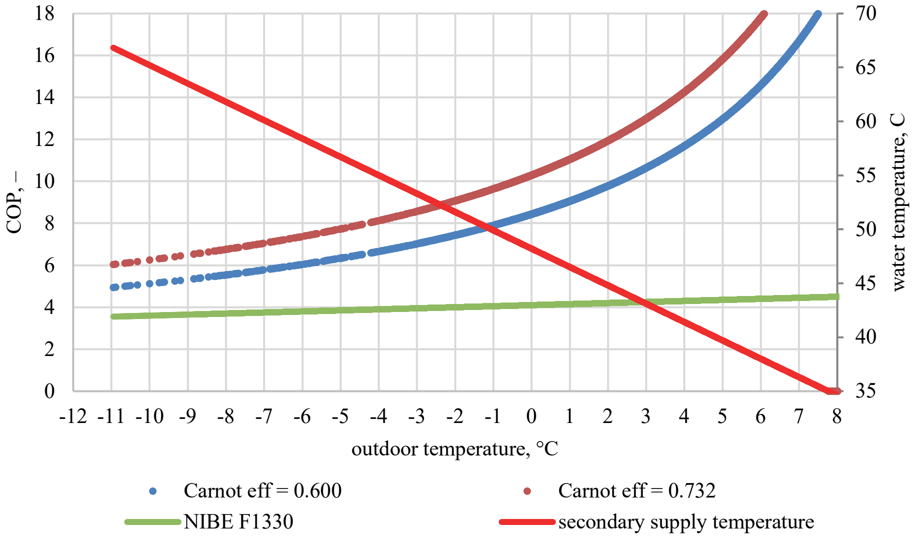

Fig. 5. COP variation of a booster heat pump compared to a traditional ground source heat pump (NIBE F1330 from [26] is used as a benchmark).

TABLE 2. COST COMPONENT COMPARISON

Value	Unit	Scenario#1	Scenario#2	Change
Carnot eff	n/a	0.600	0.732	+22 %
SCOP	n/a	5.1	6.2	+22 %
OpEx	MEUR/yr	1.55	1.27	–18 %
CapEx	kEUR/yr	61.8	92.8	+50 %
Total	MEUR/yr	1.610	1.362	–11 %

The electricity consumption for the business-as-usual scenario is assessed as described in the M&M section with an average seasonal COP of 5.1 and heat demand of 23.9 GWh/year. In the calculations, 1.7 as a slope and 16 °C as an indoor temperature were used. It is pretty conservative based on the assumption of considering an efficient space heating system in a newly built office building with an average winter temperature of 50 °C. According to the simulations, the COP was about 6.0 in winter conditions and about 12.0 in the transition period.

Peak heat demand is 12.0 MW, covered by the 5GDHC network and 25 booster water-to-water heat pumps with an average power of 478 kW each. Both network and secondary supply temperatures affect COP by considering a 5 ºC pinch applied to the reference temperatures reported for the booster heat pumps (which are assumed to be in operation when the required secondary supply temperatures are higher than the temperature in the warm pipe of the network), and no heat is then lost to the environment. The minimum secondary supply temperature set as a condenser temperature is 36 °C. These conditions lead to a max COP of 17.8 for a Tout of +7.44 °C.

The correlation between outdoor temperature, secondary supply temperature, and COP is described by Eq. (1) and Eq. (3) where η_{HP} is the efficiency of an ideal Carnot cycle in the associated scenario and with no part-load negative effect. As initial η_{HP}, a constant value of 0.6 for every HP is set. Therefore, the novel heat pump has an efficiency of 0.732 (0.6 + 22 %).

The designed 5GDHC system, coupled with the renewable energy plant and public grid, ensures 0.33 EUR/kWh set as the primary energy price and no fines for CO_2 emissions, with a project life span of 20 years. The energy production (incl. those with the help of decentralized renewables, thermal energy storage, and waste heat) meets the neighborhood's total heat demand at any time step, while 100 % of the consumed electric energy is converted into heat. The high SCOP values of the heat pumps are assessed strictly for the two modes (off and on). Mode 'booster heat pump off' is possible in case of heat exchange with network water, whose temperature is fixed at 35 °C. The only reason for the improvement between scenarios is the rise of Carnot's efficiency. That results in SCOP of 14.8 (for Scenario#1) and 18.1 (for Scenario#2). All the values are obtained for one particular case study location, with the total areas of office buildings connected set to 79 720 m^2.

The gradual conversion to novel heat pumps results in an increased CapEx cost but decreases OpEx costs. That results in the reduction of the total costs by 11 % for a new scenario that is reasoned to an 18 % decrease in OpEx despite a 50 % increase in CapEx.

5. DISCUSSION

To compare, by applying the parameters illustrated in [2] and the hourly energy demand as follows: seasonal COP of 3.3 and the annual heat demand of 628 MWh, two design configurations were compared with respect to the borehole component of a GSHP. To do it, Viesi *et al.* [2] used EED software with the limiting depth of the boreholes set to 150 m for the 1st scenario and 200 m for the 2nd scenario.

In [27], a value of 3.0 was used as the COP obtained as the result of long-term parameter measurements of the EAHP system in a newly built apartment building. Based on the measurements, the COP was about 3.0 in winter conditions and about 3.3 in the transition period. This assessment is pretty conservative and does not reflect any improvement in the thermodynamic cycle.

The authors previously considered a system including two heat pumps of 240 kW each to ensure an installed capacity of 480 kW [20]. At that time, the focus was on the heat exchange surface areas affecting COP by considering the 15%-safety factor. However, for the COP of a booster heat pump, a very conservative estimate of 4 was given.

Most of the new heat pumps use R-410A refrigerant as a working medium. As a benchmark for these heat pump models, Lammle *et al.* [23] choose market-average heat pumps with a rated efficiency of 3.8 for the air-source and 4.9 for the ground-source ones.

In [15], the gradual conversion to individual heat pumps increases the OpEx component but decreases the adverse environmental effect. They suggest an optimal configuration, for which an installed capacity of solar panels was set to 26 MW, and 36 MW wind turbines are constructed. All of these are relevant for the scenario, implying covering 10 % of the heat demand with the help of the DH system. For more optimistic scenarios, 24 and 33 MW PV panels are required. In [4], to get a smaller payback period, a PV field even larger than 200 000 m^2 is necessary.

Quirosa *et al*. [14] present seasonal COP of the same magnitude for the novel heat pump operating in similar conditions (5.09). The increase of COP due to the technology improvement is 12 % less intensive compared to those induced by transition from 3GDH to 4GDH concept (from 2.9 to 3.9) reported in [5]. Al-Sayyab *et al*. [8] also provide the correlation between condenser temperature and the COP, which achieves a maximum of 5.0 at the condenser temperature of 35 °C. Pasqui *et al*. [11] also present COP for different condenser temperatures. The same with Fig. 6, COP is the lowest for the secondary supply temperature of 60 °C, but is the highest for 35 °C. However, an upper threshold of 5.0 for any temperature is set in that paper. Stanica *et al*. [28] use a similar correlation between secondary supply temperature and outdoor temperature, which results in a similar correlation as described in Fig. 5.

6. CONCLUSION

Two thermodynamic configurations were tested and applied to a real neighbourhood, provided that they cannot interfere with or affect the results for a fixed set of the input parameters recommended for the large 5DGHC with several booster heat pumps. Hereby, 2 scenarios studied for the normal winter conditions with emitter temperatures of up to 60 °C and network temperature of 35 °C indicate an improvement of 22 % in SCOP and –18 % in electricity consumption. The positive effect for the system is possible thanks to the better energy and environmental performance despite the increase in the yearly capital costs (from 61.8 to 92.8 kEUR/yr). The main implication of the research is to support the increase in the capacity and energy production of individual electricity-driven heat pumps. With the temperature difference between the condenser/emitter temperature and water absorbing or releasing the heat fixed as a pinch for the same heat exchange area of the condenser, a booster heat pump becomes more efficient, which increases all the indicators of the 5GDHC system. For future research, a variation with almost complete conversion to decentralized heat pumps is suggested, which means only technologies with the highest power-to-heat ratio should remain. With the increased energy supply from renewables, it is now possible to further decrease the energy price while lowering both carbon emissions and system costs, as already presented in this paper.

ACKNOWLEDGEMENT

This project received funding from VLAIO in Belgium, ICON project OPTIMESH (VLAFLX7, https://researchportal.vub.be/en/projects/icon-project-optimesh & FLUX50 ICON Project Collaboration Agreement - HBC.2021.0395).

REFERENCES

[1] Gong Y., Ma G., Jiang Y., Wang L. Research progress on the fifth-generation district heating system based on heat pump technology. *Journal of Building Engineering* 2023:71:106533. https://doi.org/10.1016/j.jobe.2023.106533

[2] Viesi D., Galgaro A., Santa D. G., Sipio D. E., Garbari T., Visintainer P., Zanetti A., Sassi R., Crema L. Combining geological surveys, sizing tools and 3D multiphysics in designing a low temperature district heating with integrated ground source heat pumps. *Geothermics* 2022:101:102381. https://doi.org/10.1016/j.geothermics.2022.102381

[3] Pursiheimo E., Lindroos T. J., Sundell D., Rämä M., Tulkki V. Optimal investment analysis for heat pumps and nuclear heat in decarbonised Helsinki metropolitan district heating system. *Energy Storage and Saving* 2022:1(2):80–92. https://doi.org/10.1016/j.enss.2022.03.001

[4] Calise F., Liberato Cappiello F., Cimmino L., Dentice d'Accadia M., Vicidomini M. Optimal design of a 5th generation district heating and cooling network based on seawater heat pumps. *Energy Conversion and Management* 2022:267:2022. https://doi.org/10.1016/j.enconman.2022.115912

[5] Sorknæs P., Nielsen S., Lund H., Mathiesen V. B., Moreno D., Thellufsen Z. J. The benefits of 4th generation district heating and energy efficient datacentres. *Energy* 2022:260:125215. https://doi.org/10.1016/j.energy.2022.125215

[6] Cozzini M., Bava F. Integration of Substations into DHC Networks 2018.

[7] Brunt N., Duquette J., O'Brien W. Techno-economic and environmental performance of two state-of-the-art solar-assisted district energy system topologies. *Energy* 2023:276:127638. https://doi.org/10.1016/j.energy.2023.127638

[8] Al-Sayyab A. K. S., Navarro-Esbrí J., Mota-Babiloni A. Energy, exergy, and environmental (3E) analysis of a compound ejector-heat pump with low GWP refrigerants for simultaneous data center cooling and district heating. *International Journal of Refrigeration* 2022:133:61–72. https://doi.org/10.1016/j.ijrefrig.2021.09.036

[9] Dino G. E., Catrini P., Buscemi A., Piacentino A., Palomba V., Frazzicia A. Modeling of a bidirectional substation in a district heating network: Validation, dynamic analysis, and application to a solar prosumer. *Energy* 2023:284:128621. https://doi.org/10.1016/j.energy.2023.128621

[10] Capone M., Guelpa E., Verda V. Optimal Installation of Heat Pumps in Large District Heating Networks. *Energies (Basel)* 2023:16(3):1448. https://doi.org/10.3390/en16031448

[11] Pasqui M., Vaccaro G., Lubello P., Milazzo A., Carcasci C. Heat pumps and thermal energy storages centralised management in a Renewable Energy Community. *International Journal of Sustainable Energy Planning and Management* 2023:38:65–82. https://doi.org/10.54337/ijsepm.7625

[12] Maccarini A., Sotnikov A., Sommer T., Wetter M., Sulzer M., Afshari A. Influence of building heat distribution temperatures on the energy performance and sizing of 5th generation district heating and cooling networks. *Energy* 2023:275:127457. https://doi.org/10.1016/j.energy.2023.127457

[13] Martinazzoli G., Pasinelli D., Lezzi A. M., Pilotelli M. Design of a 5th Generation District Heating Substation Prototype for a Real Case Study. *Sustainability* 2023:15(4):2972. https://doi.org/10.3390/su15042972

[14] Quirosa G., Torres M., Soltero V. M., Chacartegui R. Energetic and economic analysis of decoupled strategy for heating and cooling production with CO_2 booster heat pumps for ultra-low temperature district network. *Journal of Building Engineering* 2022:45:103538. https://doi.org/10.1016/j.jobe.2021.103538

[15] Johannsen R. M., Prina M. G., Østergaard P. A., Mathiesen B. V., Sparber W. Municipal energy system modelling – A practical comparison of optimisation and simulation approaches. *Energy* 2023:269:126803. https://doi.org/10.1016/j.energy.2023.126803

[16] Frik A., Bielskus J., Dzikevics M. Experimental Study on the Control of the Positions of the Cycle Isotherms of the Heat Pump in the Air Handling Unit. *Environmental and Climate Technologies* 2023:27(1):889–899. https://doi.org/10.2478/rtuect-2023-0065

[17] Ołtarzewska A., Krawczyk D. A. Analysis of Heat Pumps Efficiency in Selected Locations – A Case Study. *Environmental and Climate Technologies* 2022:26(1):648–657. https://doi.org/10.2478/rtuect-2022-0049

[18] Kirs T., Sukumaran S., Latõšov E., Volkova A. Use of Absorption Heat Pumps to Raise District Cooling Waste Heat Temperature for District Heating Supply in Tallinn: Technical and Economic Analysis. *Environmental and Climate Technologies* 2024:28(1):409–421. https://doi.org/10.2478/rtuect-2024-0032

[19] Arabkoohsar A., Alsagri A. S. A new generation of district heating system with neighborhood-scale heat pumps and advanced pipes, a solution for future renewable-based energy systems. *Energy* 2020:193:116781. https://doi.org/10.1016/j.energy.2019.116781

[20] Chicherin S., Zhuikov A., Junussova L. Integrating a heat pump into a 4th generation district heating (4GDH) system – Two-mode configuration inputting operational data. *Energy and Buildings* 2022:275:112445. https://doi.org/10.1016/j.enbuild.2022.112445

[21] Serrat L., Linares J. I., Cledera M. M., Morales C., Hueso K. Ground source heat pump driven by reciprocating engine firing biomethane from wastewater treatment plant sludge in a cogeneration for district heating and cooling. A case study in Spain. *Applied Thermal Engineering* 2023:219:119586. https://doi.org/10.1016/j.applthermaleng.2022.119586

[22] Hering D., Cansev M. E., Tamassia E., Xhonneux A., Müller D. Temperature control of a low-temperature district heating network with Model Predictive Control and Mixed-Integer Quadratically Constrained Programming. *Energy* 2021:224:120140. https://doi.org/10.1016/j.energy.2021.120140

[23] Lämmle M., Bongs C., Wapler J., Günther J., Hess S., Kropp M., Herkel S. Performance of air and ground source heat pumps retrofitted to radiator heating systems and measures to reduce space heating temperatures in existing buildings. *Energy* 2022:242:122952. https://doi.org/10.1016/j.energy.2021.122952

[24] Jebamalai J. M., Marlein K., Laverge J. Influence of centralized and distributed thermal energy storage on district heating network design. *Energy* 2020:202:117689. https://doi.org/10.1016/j.energy.2020.117689

[25] How to use your heat pump efficiently this winter. Genesis NZ [Online]. Available: https://www.genesisenergy.co.nz/tips-and-tricks/articles/use-your-heat-pump-efficiently-this-winter

[26] Lygnerud K., Ottosson J., Kensby J., Johansson L. Business models combining heat pumps and district heating in buildings generate cost and emission savings. *Energy* 2021:234:121202. https://doi.org/10.1016/j.energy.2021.121202

[27] Korpela T., Kuosa M., Sarvelainen H., Tuliniemi E., Kiviranta P., Tallinen K., Koponen H. K. Waste heat recovery potential in residential apartment buildings in Finland's Kymenlaakso region by using mechanical exhaust air ventilation and heat pumps. *International Journal of Thermofluids* 2022:13:100127. https://doi.org/10.1016/j.ijft.2021.100127

[28] Stanica D. I., Bachmann M., Kriegel M. Design and performance of a multi-level cascading district heating network with multiple prosumers and energy storage. *Energy Reports* 2021:7(S4):128–139. https://doi.org/10.1016/j.egyr.2021.08.163